On partially integrated transport models for subgrid-scale modeling

Roland Schiestel*
IRPHE, Château-Gombert, 13384 Marseille, France

Bruno Chaouat**
ONERA , 92322 Châtillon, France

1 Context and issues

Mathematical turbulence modelling methods have made significant progress in the past decade for predicting various practical turbulent shear flows. Many different types of models have been developed in the past, such as RANS (Reynolds-averaged Navier-Stokes) models [1, 2]. Generally, the RANS models appear well suited to handle engineering applications involving strong effects of streamline curvature, system rotation, wall injection or adverse pressure gradient encountered for instance in aeronautics applications [3, 4, 5, 6]. Multiple-scale models [7, 8, 9] have been developed to account for spectral non-equilibrium in the framework of one-point closures. Others works [10, 11] have been made then in this framework. Important works have been also devoted to the two-point approach to extend these closures to the case of non-homogeneous turbulence. After the work of Cambon et al. [12] dealing with the extension of EDQNM (eddy-damped quasi-normal Markovian) closures, several efforts have been pursued [13]. On the other hand, as shown for instance by Lesieur [14], the LES (large eddy simulations) method using subgrid modelling techniques [15, 16] favoured by the continuous increase in computer power and speed has been extensively developed. All these various approaches have often been developed along independent lines and the connection between them is generally not clearly established. So, there is a real need to unify these points of view in a coherent manner in order to easily bridge these apparently different models [17]. In this line of thought, let us mention that recently, new turbulence models that take advantage of RANS and LES approaches based on hybrid zonal methods [18, 19, 20] or on a hybrid continuous method with "seamless coupling " [21, 22] are now currently developed for simulating practical turbulent flows. These models are useful for calculations on relatively coarse grids when the spectral cutoff is located before the inertial zone. The hybrid continuous method [21, 22] presents major interest on a fundamental point of view because it bridges different levels of description

*Senior Scientist, CNRS. E-mail address: Roland.Schiestel@irphe.univ-mrs.fr
**Senior Scientist, ONERA. E-mail address: Bruno.Chaouat@onera.fr

in a consistent way [23]. With a particular emphasis upon the connection between RANS and LES, we shall show in this paper how the continuous hybrid formulation can be developed. This method is based on the spectral Fourier transform of the two-point fluctuating velocity correlation equations with an extension to nonhomogeneous turbulence [17]. In particular, the partial integration based on spectrum splitting, gives rise to PITM method (partial integrated transport models) [21, 22]. This approach can yield subfilter transport models that can be used in LES or in hybrid methods, providing some appropriate approximations are made. The method is well appropriate for calculating non-equilibrium turbulent flows. In this paper, some applications will be then considered for illustrating the potentials of this approach.

In the present paper, we shall rely upon a theoretical method based on mathematical physics formalism to allow transposition of turbulence modelling from RANS to LES [17]. The recent scientific literature shows increasing interest in the use of more advanced models in subgrid-scale closures, including subfilter algebraic stress models or stress transport models inspired from RANS [24]. This can be related also to the hybrid RANS/LES approach with seamless coupling [20, 23].

2 PITM approach to subgrid-scale turbulence models

2.1 General formalism

As usually made in large eddy simulations, the spectrum is then portioned using a cutoff wave number κ_c. In classical LES this cutoff is located in the beginning of the inertial range of eddies but in the present approach, like in very large eddy simulations, the cutoff may be located before the inertial range. For convenience, another wave number κ_d located at the end of the inertial range of the spectrum can also be used, assuming that the energy pertaining to higher wavenumbers is entirely negligible. This practise avoids considering infinite limits and molecular viscosity effects in the far end of the spectrum. When non-homogeneous turbulence is considered (this is the usual case), the concept of tangent homogeneous space at a point of the non-homogeneous flow field must be used. In this case, it is then possible to define the large scale fluctuations (resolved scales) $u_i^<$ and the fine scales (modelled scales) $u_i^>$ through the relations using the wave number $\boldsymbol{\kappa}$

$$u_i^< = \int_{|\boldsymbol{\kappa}| \leq \kappa_c} \widehat{u'}_i(\boldsymbol{X}, \boldsymbol{\kappa}) \exp\left(j \boldsymbol{\kappa} \boldsymbol{\xi}\right) \, d\boldsymbol{\kappa} \tag{1}$$

$$u_i^> = \int_{|\boldsymbol{\kappa}| \geq \kappa_c} \widehat{u'}_i(\boldsymbol{X}, \boldsymbol{\kappa}) \exp\left(j \boldsymbol{\kappa} \boldsymbol{\xi}\right) \, d\boldsymbol{\kappa} \tag{2}$$

If large eddy simulations make use of a filtering operation instead of statistical averaging, it is of interest to remark that the previous definition is indeed a filter operating in Fourier space. But it is a particular filter with interesting properties : if integration is performed in $\boldsymbol{\kappa}$ in the tangent homogeneous space, then, the quantity obtained becomes a function of $\boldsymbol{X}$, and it is the usual statistical mean (see figure 1). So, the previous filter, sometimes called the statistical filter, is well suited to bridge RANS and

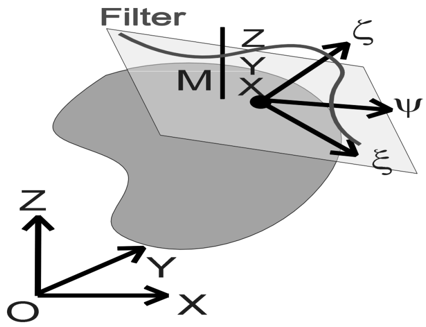

Figure 1: Sketch of tangent homogeneous space hypothesis

LES. Then, the instantaneous velocity u_i can be decomposed into a statistical part $\langle u_i \rangle$, a large scale fluctuating $u_i^<$ and a small scale fluctuating $u_i^>$ such that $u_i = \langle u_i \rangle + u_i^< + u_i^>$. The first two terms correspond to the filtered velocity $\bar{u}_i$ such that $\bar{u}_i = \langle u_i \rangle + u_i^<$. The velocity fluctuation u_i' contains a large-scale and a small-scale parts, $u_i' = u_i^< + u_i^>$. This particular filter, as a spectral truncation, presents also some additional useful properties that are not verified for progressive filters. In particular, it can be shown [8] that large scale and small scale fluctuations are uncorrelated $\langle \varphi^> \psi^< \rangle = 0$ implying for instance the relation

$$R_{ij} = \langle u_i u_j \rangle - \langle u_i \rangle \langle u_j \rangle = \langle u_i' u_i' \rangle = \left\langle u_i^< u_j^< \right\rangle + \left\langle u_i^> u_j^> \right\rangle \tag{3}$$

The transport equation for the filtered Navier-Stokes equations takes the form

$$\frac{\partial \bar{u}_i}{\partial t} + \frac{\partial}{\partial x_j} \left(\bar{u}_i \bar{u}_j \right) = -\frac{1}{\rho} \frac{\partial \bar{p}}{\partial x_i} + \nu \frac{\partial^2 \bar{u}_i}{\partial x_j \partial x_j} - \frac{\partial \tau_(u_i, u_j)}{\partial x_j} \tag{4}$$

in which, following Germano's derivation [25], the subgrid-scale tensor is defined by the relation

$$(\tau_{ij})_{sgs} = \tau(u_i, u_j) = \overline{u_i u_j} - \bar{u}_i \bar{u}_j \tag{5}$$

The work of Germano [25] shows that the transport equation for the subgrid-scale tensor takes a generic form if it is written in terms of central moments. The resulting equation can be rearranged as

$$\begin{aligned} \frac{\partial \tau(u_i, u_j)}{\partial t} + \frac{\partial}{\partial x_k} \left[\tau(u_i, u_j) \bar{u}_k \right] = \\ -\tau(u_i, u_k) \frac{\partial \bar{u}_j}{\partial x_k} - \tau(u_j, u_k) \frac{\partial \bar{u}_i}{\partial x_k} \\ +\tau \left(p, \frac{\partial u_i}{\partial x_j} + \frac{\partial u_j}{\partial x_i} \right) \\ -\frac{1}{\rho} \frac{\partial \tau(p, u_i)}{\partial x_j} - \frac{1}{\rho} \frac{\partial \tau(p, u_j)}{\partial x_i} - \frac{\partial \tau(u_i, u_j, u_k)}{\partial x_k} \\ +\nu \frac{\partial^2 \tau(u_i, u_j)}{\partial x_k \partial x_k} - 2\nu \tau \left(\frac{\partial u_i}{\partial x_k}, \frac{\partial u_j}{\partial x_k} \right) \end{aligned} \tag{6}$$

with the general definition $\tau(f,g) = \overline{fg} - \bar{f}\bar{g}$ and $\tau(f,g,h) = \overline{fgh} - \bar{f}\tau(g,h) - \bar{g}\tau(h,f) - \bar{h}\tau(f,g) - \bar{f}\bar{g}\bar{h}$ for any turbulent quantities f, g, h. Equation (6) will then be solved numerically in space and time. This equation is fluctuating but has a similar form as the equations used in statistical multiple scale models [17]. Using the definition $D/Dt = \partial/\partial t + \bar{u}_k \partial/\partial x_k$, equation (6) reads

$$\frac{D(\tau_{ij})_{sgs}}{Dt} = (P_{ij})_{sgs} + (\Psi_{ij})_{sgs} + (J_{ij})_{sgs} - (\epsilon_{ij})_{sgs} \tag{7}$$

where in this equation, the production term $(P_{ij})_{sgs}$ is

$$(P_{ij})_{sgs} = -(\tau_{ik})_{sgs}\frac{\partial \bar{u}_j}{\partial x_k} - (\tau_{jk})_{sgs}\frac{\partial \bar{u}_i}{\partial x_k} \tag{8}$$

The corresponding equation for subfilter energy is obtained by the half trace

$$\frac{Dk_{sgs}}{Dt} = P_{sgs} + J_{sgs} - \epsilon_{sgs} \tag{9}$$

where $P_{sgs} = (P_{mm})_{sgs}/2$ and $\epsilon_{sgs} = (\epsilon_{mm})_{sgs}/2$. Because of the nice properties of the truncation filter in Fourier space, the mean statistical and filtered equations can both be written in a similar form. As a consequence, we shall assume that closure approximations used for the statistical partially averaged equations also prevail in the case of large eddy numerical simulations. Let us mention that the present formalism is in fact the essence of the PITM model, first developed by Schiestel and Dejoan [21] for the transport equation (9) of the subgrid-scale turbulent energy $k_{sgs} = (\tau_{mm})_{sgs}/2$ and subsequently by Chaouat and Schiestel [22] for the transport equation (7) of the subgrid-scale turbulent stress tensor $(\tau_{ij})_{sgs}$.

2.2 Two-equation subfilter model

For LES or hybrid RANS/LES approaches, this level of closure is composed of an equation for subfilter turbulence energy coupled with a dissipation rate equation. The transport equation of the dissipation rate used in subfilter models is somewhat different from the equation usually used in statistical models. In the tangent homogeneous space, the value of the mean velocity gradient is denoted Λ_{ij}. The equation of the energy spectrum balance $E(\kappa)$ can be obtained by taking the Fourier transform and mean value on spherical shells of the transport equation of the two-points velocity correlation [8, 26]:

$$\frac{\partial E}{\partial t} = -\Lambda_{ij}\tau_{ij} + T - 2\nu\kappa^2 E \tag{10}$$

Integration of the basic equation (10) over the wave number range $[\kappa_c, \kappa_d]$, where κ_c is the cutoff wave number given by the filter width and κ_d is the splitting wave number (see figure 2), yields at high Reynolds numbers

$$\frac{\partial \langle k_{gs}\rangle}{\partial t} = \langle P_{sgs}\rangle - F(\kappa_d) + F(\kappa_c) - \epsilon \tag{11}$$

with the relations

$$\langle k_{sgs} \rangle = \int_{\kappa_c}^{\kappa_d} E(\kappa) d\kappa \tag{12}$$

$$\langle P_{sgs} \rangle = -\Lambda_{lm} \int_{\kappa_c}^{\kappa_d} \tau_{lm}(\kappa) d\kappa \tag{13}$$

$$F(\kappa) = \mathcal{F}(\kappa) - E(\kappa) \frac{\partial \kappa}{\partial t} \tag{14}$$

$$\mathcal{F}(\kappa) = \int_{\kappa}^{\infty} T(\kappa') d\kappa' = -\int_{0}^{\kappa} T(\kappa') d\kappa' \tag{15}$$

$$\epsilon = 2\nu \int_{\kappa_c}^{\kappa_d} \kappa^2 E(\kappa) d\kappa \tag{16}$$

$\mathcal{F}$ represents the spectral energy rate transferred into the wave number range $[\kappa, +\infty]$ by vortex stretching from the wave number range $[0, \kappa]$. Equation (9) can be derived equivalently in physical space [22] with corresponding expressions for the production, transfer and dissipation (9). Considering the cutoff wave number κ_c given by the filter width, the splitting wave number κ_d is then determined by the dimensional relation

$$\kappa_d - \kappa_c = \zeta_c \frac{\epsilon}{\langle k_{sgs} \rangle^{3/2}} \tag{17}$$

where ζ_c is a coefficient which may be dependent on the spectrum shape and on the Reynolds number. Note that this relation is identical to the relation introduced in statistical multiple scale models [9]. The net flux across the splitting wavenumber κ_d, due to the variations of the splitting is related to the usual spectral flux by equation (14). As a consequence we obtain

$$\frac{\partial \kappa_d}{\partial t} = \frac{\mathcal{F}(\kappa_d) - F(\kappa_d)}{E(\kappa_d)} \tag{18}$$

Taking into account equation (18) one can easily obtain the transport equation for the dissipation rate

$$\frac{\partial \epsilon}{\partial t} = c_{sgs\epsilon_1} \frac{\epsilon}{\langle k_{sgs} \rangle} \left(\langle P_{sgs} \rangle + F(\kappa_c) \right) - c_{sgs\epsilon_2} \frac{\epsilon^2}{\langle k_{sgs} \rangle} \tag{19}$$

where $c_{sgs\epsilon_1} = 3/2$ and

$$c_{sgs\epsilon_2} = \frac{3}{2} - \frac{\langle k_{sgs} \rangle}{\kappa_d E(\kappa_d)} \left(\frac{\mathcal{F}(\kappa_d)}{\epsilon} - 1 \right) \tag{20}$$

setting $\kappa_d \gg \kappa_c$, and $E(\kappa_d) \ll E(\kappa_c)$. In the case of full statistical modelling where $\kappa_c = 0$, equation (17) is reduced to the equation:

$$\kappa_d = \zeta_d \frac{\epsilon}{k^{3/2}} \tag{21}$$

where the coefficient ζ_d is a numerical constant chosen such that κ_d is located after the inertial range. By taking the derivative of equation (21) with respect to time, using equation (18) , another formulation of the standard dissipation rate equation is then obtained

$$\frac{\partial \epsilon}{\partial t} = c_{\epsilon_1} \frac{\epsilon}{k} P - c_{\epsilon_2} \frac{\epsilon^2}{k} \tag{22}$$

where $c_{\epsilon_1} = 3/2$ and

$$c_{\epsilon_2} = \frac{3}{2} - \frac{k}{\kappa_d E(\kappa_d)} \left(\frac{\mathcal{F}(\kappa_d)}{\epsilon} - 1 \right) \tag{23}$$

This is in fact the usual ϵ equation used in statistical closures. Equations (20) and (23) show that the coefficients $c_{sgs\epsilon_1}$ and $c_{sgs\epsilon_2}$ are functions of the spectrum shape. Keeping in mind that the dissipation rate ϵ must remain the same regardless the location of the wave number κ_c, comparing equation (19) with equation (22) allows to express the coefficient $c_{sgs\epsilon_2}$ in a more convenient form

$$c_{sgs\epsilon_2} = c_{\epsilon_1} + \frac{\langle k_{sgs} \rangle}{k} (c_{\epsilon_2} - c_{\epsilon_1}) \tag{24}$$

2.3 Model calibration

The function $\langle k_{sgs} \rangle / k$ which appears in equation (24) can be calibrated by referring to the Kolmogorov law of the three-dimensional energy spectrum in the inertial wave number range in nearly equilibrium flows $E(\kappa) = C_K \epsilon^{2/3} \kappa^{-5/3}$ where $C_K \approx 1.50$ is the Kolmogorov constant. The subgrid-scale turbulent kinetic energy is then estimated by integrating the Kolmogorov law in the wave number range $[\kappa_c, +\infty[$

$$\langle k_{sgs} \rangle = \int_{\kappa_c}^{\infty} E(\kappa) d\kappa = \frac{3}{2} C_K \epsilon^{2/3} \kappa_c^{-2/3} \tag{25}$$

Introducing a dimensionless wave number defined by $\eta_c = \kappa_c k^{3/2}/(\epsilon + \epsilon^<)$ where $\epsilon^< = \nu \partial u_i^< \partial u_i^< / \partial x_j \partial x_j$ represents the small part of dissipation coming from the resolved scales $u_i^<$, and taking into account equation (25), we obtain $k_{sgs}/k = 1.5\, C_K \eta_c^{-2/3}$. The statistical kinetic energy $k = \langle k_{sgs} \rangle + \langle k_{les} \rangle$ is the total turbulence energy. As it was mentioned, the total dissipation rate $\epsilon + \epsilon^<$ includes now the usual part caused by the subgrid-scale fluctuating and the small part coming from the resolved scales fluctuating in order to represent the characteristic scale of the whole turbulence spectrum. As found, the function $\langle k_{sgs} \rangle / k$ is dependent of the parameter $\eta_c^{-2/3}$. However, this previous result is only valid in the inertial range. It is extended empirically to the general case, taking care to satisfy the limit when $\langle k_{sgs} \rangle$ tends to k, (i.e. when η_c goes to zero). So, the coefficient $c_{sgs\epsilon_2}$ in equation (24) is modelled as follows

$$c_{sgs\epsilon_2} = c_{\epsilon_1} + \frac{c_{\epsilon_2} - c_{\epsilon_1}}{1 + \beta_\eta \, \eta_c^{2/3}} \tag{26}$$

where β_η is a numerical constant which takes the theoretical value $\beta_\eta = 2/3C_K \approx 0.444$ in order to satisfy the correct asymptotic behaviour in $\eta_c^{-2/3}$ for high values η_c with the limiting conditions:

$\lim_{\eta_c \to 0} c_{sgs\epsilon_2}(\eta_c) = c_{\epsilon_2}$, $\lim_{\eta_c \to \infty} c_{sgs\epsilon_2}(\eta_c) = c_{\epsilon_1}$. In the limit of full statistical modelling, $\langle k_{sgs} \rangle \to k$ and the usual RSM model is recovered while in the limit $\langle k_{sgs} \rangle \to 0$, the subgrid-scale energy is not maintained due to the fact that $c_{sgs\epsilon_2} \to c_{\epsilon_1}$ and the model behaves like a DNS (but the model become useless!). The instantaneous fluctuating dissipation rate ϵ_{sgs} verifies the relation $\langle \epsilon_{sgs} \rangle = \epsilon$. For LES, we propose a modelled transport equation for the fluctuating dissipation rate ϵ_{sgs}, referring to equation (19). Taking into account the convective and diffusive processes as well as low Reynolds number terms for non-homogeneous flows, the fluctuating dissipation rate ϵ_{sgs} then reads

$$\frac{D\epsilon_{sgs}}{Dt} = c_{\epsilon_1} \frac{\epsilon_{sgs}}{k_{sgs}} \frac{(P_{mm})_{sgs}}{2} - c_{sgs\epsilon_2} \frac{\widetilde{\epsilon}_{sgs}\epsilon_{sgs}}{k_{sgs}} + (J_\epsilon)_{sgs} \tag{27}$$

where

$$(J_\epsilon)_{sgs} = \frac{\partial}{\partial x_j} \left(\left(\nu + \frac{\nu_{sgs}}{\sigma_\epsilon} \right) \frac{\partial \epsilon_{sgs}}{\partial x_j} \right) \tag{28}$$

and $\widetilde{\epsilon}_{sgs} = \epsilon_{sgs} - 2\nu \left(\partial \sqrt{k_{sgs}} / \partial x_n \right)^2$. The values of the numerical coefficients in equations (26) and (27) are $c_{\epsilon_1} = 1.45$, $c_{\epsilon_2} = 1.9$ and $\sigma_\epsilon = 1.3$.

2.4 Practical formulation

The two equation subfilter model is composed of the modelled equations (9) and (27) together with a gradient diffusion hypothesis $\nu_{sgs} = c_\nu k_{sgs}^2 / \epsilon_{sgs}$. In a practical formulation for the case of wall bounded flows, the length scale can be computed using the normal distance to the wall $L = K x_3$ where K is the Von Kármán constant. In that condition, we use the alternative dimensionless wave number $\mathcal{N}_c = \kappa_c L$ instead of η_c and we introduce the modified coefficient $\beta_\mathcal{N}$ in equation (26). In that framework, the alternative functions of the subgrid-scale turbulence model are written equivalently with $\beta_\eta \, \eta_c^{2/3} = \beta_\mathcal{N} \mathcal{N}_c^{2/3}$. The order of magnitude of the new coefficient $\beta_\mathcal{N}$ is then obtained by reference to the logarithmic layer leading to the theoretical value $\beta_\mathcal{N} \approx 1.466$. The cutoff wave number is approximated by the filter width $\kappa_c = \pi / (\Delta_1 \Delta_2 \Delta_3)^{1/3}$.

2.5 Limiting behaviour

With the tangent homogeneous space in mind, let us remark finally that when very large filter widths are used, the filter width has to be dissociated from the grid itself, because the grid must always be fine enough to capture the mean flow non-homogeneities. When the cutoff location is large then, limiting behaviours are obtained. The length scale $k_{sgs}^{3/2} / \epsilon_{sgs}$ is equal to

$$\frac{k_{sgs}^{3/2}}{\epsilon_{sgs}} = \frac{k^{3/2}}{\epsilon_{sgs}} \left(\frac{k_{sgs}}{k} \right)^{3/2} \tag{29}$$

Taking into account the preceding expression of $\langle k_{sgs} \rangle / k$, equation (29) shows that the subgrid characteristic length scale goes to the filter width

$$k_{sgs}^{3/2} / \epsilon_{sgs} = (3 C_K / 2)^{3/2} \, \Delta / \pi \tag{30}$$

Moreover, the definition of subfilter viscosity implies $\nu_{sgs}^{3/2} = c_\nu^{3/2}(k_{sgs}^3/\epsilon_{sgs}^{3/2}) = c_\nu^{3/2}\left(k_{sgs}^3/\epsilon_{sgs}^2\right)\epsilon_{sgs}^{1/2}$ or $\nu_{sgs} = c_\nu^{3/2}\left(k_{sgs}^3/\epsilon_{sgs}^2\right)(\epsilon_{sgs}/\nu_{sgs})^{1/2}$. Using then the previous result on the length scale together with the hypothesis of equilibrium $\epsilon_{sgs} = 2\nu_{sgs}\langle S_{i,j}S_{i,j}\rangle$ where $S_{ij} = (\partial u_i/\partial x_j + \partial u_j/\partial x_i)/2$, one finds that the limiting behaviour for the subgrid viscosity ν_{sgs} is simply the Smagorinsky model

$$\nu_{sgs} = \frac{1}{\pi^2}\left(\frac{3C_K}{2}\right)^3 c_\nu^{3/2}\Delta^2\left[2\langle S_{ij}S_{ij}\rangle\right]^{1/2} \tag{31}$$

2.6 Stress transport equation subfilter model

In the subfilter models, as usual in statistical approaches, the redistribution term $(\Psi_{ij})_{sgs}$ which appears in equation (7) is decomposed into a slow and a rapid part $(\Psi_{ij}^1)_{sgs}$ and $(\Psi_{ij}^2)_{sgs}$ in the subgrid-scale range. The slow term is modelled assuming that usual statistical Reynolds stress models must be recovered in the limit of vanishing cutoff wave number κ_c and also that the return to isotropy is increased at higher wave numbers [22], as also assumed in multiple-scale models

$$(\Psi_{ij}^2)_{sgs} = -c_{sgs_1}\frac{\epsilon_{sgs}}{k_{sgs}}\left((\tau_{ij})_{sgs} - \frac{1}{3}(\tau_{mm})_{sgs}\delta_{ij}\right) \tag{32}$$

$$(\Psi_{ij}^1)_{sgs} = -c_2\left((P_{ij})_{sgs} - \frac{1}{3}(P_{mm})_{sgs}\delta_{ij}\right) \tag{33}$$

where c_{sgs_1} is now a continuous function of the cutoff wave number κ_c. The value of this coefficient can be calibrated from experiments. According to the classical physics of turbulence, the coefficient c_{sgs_1} must increase with the parameter η_c in order to increase the return to isotropy in the range of larger wave numbers. To do that, we suggest a simple empirical function

$$c_{sgs_1} = \frac{1 + \alpha_\eta\,\eta_c^2}{1 + \eta_c^2}c_1 \tag{34}$$

where α_η is a numerical constant. This function satisfies the limiting condition $\lim_{\eta_c\to 0} c_{sgs_1}(\eta_c) = c_1$. In the practical equivalent formulation, $\alpha_\eta\,\eta_c^2 = \alpha_\mathcal{N}\mathcal{N}_c^2$. In this formulation, like in the Launder and Shima model [27], the function c_1 depends on the second and third subgrid-scale invariants $A_2 = a_{ij}a_{ji}$, $A_3 = a_{ij}a_{jk}a_{ki}$ and the flatness coefficient parameter $A = 1 - \frac{9}{8}(A_2 - A_3)$ where $a_{ij} = ((\tau_{ij})_{sgs} - \frac{2}{3}k_{sgs}\delta_{ij})/k_{sgs}$. The term $(\Psi_{ij})_{sgs}$ takes into account the wall reflection effect of the pressure fluctuations and is embedded in the model for reproducing correctly the logarithmic region of the turbulent boundary layer. It is modelled according to the previous work of Gibson [28]. The diffusion process $(J_{ij})_{sgs}$ is modelled assuming a gradient law [22]

$$(J_{ij})_{sgs} = \frac{\partial}{\partial x_k}\left(\nu\frac{\partial(\tau_{ij})_{sgs}}{\partial x_k} + c_s\frac{k_{sgs}}{\epsilon_{sgs}}(\tau_{kl})_{sgs}\frac{\partial(\tau_{ij})_{sgs}}{\partial x_l}\right) \tag{35}$$

where c_s is a numerical coefficient which takes the value 0.22. Moreover, we assume $(\epsilon_{ij})_{sgs} = (2/3)\epsilon_{sgs}\delta_{ij}$. In contrast to the two-equation model, it can be mentioned that the production term $(P_{ij})_{sgs}$ is allowed to become negative. In such a case, this implies that energy is transferred from the filtered motions up to the resolved motions, known as back-scatter process. So that, the PITM model for $(\tau_{ij})_{sgs}$ and ϵ_{sgs} is based on the modelled equations (7) and (27). However, note that equation (27) is modified for the diffusion term because of its new tensorial formulation

$$(J_\epsilon)_{sgs} = \frac{\partial}{\partial x_j}\left(\nu\frac{\partial \epsilon_{sgs}}{\partial x_j} + c_\epsilon \frac{k_{sgs}}{\epsilon_{sgs}}(\tau_{jm})_{sgs}\frac{\partial \epsilon_{sgs}}{\partial x_m}\right) \tag{36}$$

In equation (36), the coefficient c_ϵ takes the value 0.18. For the limiting condition when the cutoff wave number goes to zero, one can see that the PITM model goes to the original model of Launder and Shima [27].

3 Some illustrative applications of PITM to LES and hybrid models

3.1 Non-equilibrium turbulent flows

The PITM two-equation model (9) for the subfilter turbulent kinetic energy dissipation rate has been applied to several turbulent flows including in particular the pulsed turbulent channel flow performed by Schiestel and Dejoan [21] showing occurrence of lag effects and also the turbulent shearless mixing layer by Befeno and Schiestel corresponding to the mixing of two turbulent fields of differing scales [29]. In the present paper, we shall focus mainly on injection channel flow.

3.2 Injection induced turbulent channel flow

A channel flow with mass injection through one porous wall which undergoes the development of natural unsteadiness with a transition process from laminar to turbulent regime has been performed by Chaouat and Schiestel [22]. This case is of central interest for engineering applications in solid rocket motors (SRM). The present large eddy simulation has been made using a medium grid ($400 \times 44 \times 80$) in the streamwise, spanwise and normal directions to the wall. The velocities and turbulent stress profiles are compared with experimental data [30], and also with RSM computations obtained for the limit of the PITM model when the cutoff wave number goes to zero [31, 32]. Figure 3 shows the isosurfaces of the instantaneous spanwise filtered vorticity $\bar{\omega}_2 = \partial \bar{u}_3/\partial x_1 - \partial \bar{u}_1/\partial x_3$ in the downstream part of the channel and reveals the detail of the flow structures subjected to mass injection. The isosurfaces exhibit roll-up vortex structures in the spanwise direction, indicating the transitional and turbulent flow regime. Figure 4 shows the velocity profiles $\langle u_1 \rangle / u_m$ normalised by the bulk velocity u_m in two locations of the channel at $x_1 = 40$ cm and 57 cm. It appears that both LES and RSM computations produce velocity profiles that agree rather well with the experimental data. Figure 5 describes the streamwise turbulent stresses $\langle u_1' u_1' \rangle / u_m$ in different stations of the channel at $x_1 = 40$ cm and 57 cm. As a result of interest, one can observe that both LES and RSM computations reasonably well predict the turbulence intensity of the flow in the downstream transition location where the flow presents a turbulent regime, except, however, in the immediate vicinity of the wall region.

4 Conclusion

We have shown that the partial integration concept allows to develop subfilter turbulence transport models that can be used in LES or hybrid approaches. The concept of tangent homogeneous field, considered as deriving from the first term in the Taylor development of local mean velocity field together with the use of the spectral statistical filter are essential ingredients [17]. They allow in particular to dissociate the filter from the grid itself. Because of the filtering made in the tangent space, the method can be applied in non-homogeneous flows. As known, the total integration in the tangent space exactly produces the corresponding one-point statistical model in a consistent way. This character is important for hybrid modelling applications. On the other hand, when the filter width is small, we have shown, assuming equilibrium flows, that the proposed model is equivalent to a Smagorinsky type model (of course, provided that the mesh is finer than the filter width). The PITM concept has been considered for two-equation models ($k-\epsilon$ type models) [21] and for stress transport models [22]. Obviously, every other statistical model of the scientific literature (including two-equation models, algebraic stress models, non linear models and various stress transport models) can also be transposed in subfilter version. Some applications including flow situations with non equilibrium spectrum have been then presented for illustrating some potentials of the method. The main contribution of the present approach is therefore to bridge URANS models and LES simulations, opening a promising route of new future developments in hybrid models with seamless coupling.

References

[1] G. Speziale C. Analytical methods for the development of Reynolds-stress closures in turbulence. *Annual Reviews Fluid Mechanics*, 23:107–157, 1991.

[2] B. E. Launder. Second moment closure: Present and future ? *Int. Heat and Fluid Flow*, 20(4):282–300, 1989.

[3] B. Chaouat. Reynolds stress transport modeling for high-lift airfoil flows. *AIAA Journal*, 44(10):2390–2403, 2006.

[4] M. A. Leschziner and D. Drikakis. Turbulence modelling and turbulent-flow computation in aeronautics. *The Aeronautical Journal*, 106:349–384, 2002.

[5] C. L. Rumsey and T. B. Gatski. Recent turbulence model advances applied to multielement airfoil computations. *Journal of Aircraft*, 38(5):904–910, 2001.

[6] B. Chaouat. Simulations of channel flows with effects of spanwise rotation or wall injection using a Reynolds stress model. *Journal of Fluid Engineering, ASME*, 123:2–10, 2001.

[7] K. Hanjalic, B. E. Launder, and R. Schiestel. Multiple time-scale concepts in turbulence transport modeling. In *Turbulent Shear Flows n° 2*. Ed. Springer, 1980.

[8] R. Schiestel. Sur le concept d'échelles multiples en modélisation des écoulements turbulents. *Journal de Mécanique Théorique et Appliqué,* Part I, 2, 3:417-449*;* Part II, 2, 4:601-628, 1983.

[9] R. Schiestel. Multiple-time scale modeling of turbulent flows in one point closures. *Physics of Fluids*, 30(3):722–731, 1987.

[10] T.T. Clark and C. Zemach. A spectral model applied to homogeneous turbulence. *Physics of Fluids*, 7(7):1674–1694, 1995.

[11] A. Cadiou, K. Hanjalic, and K. Stawiarski. A two-scale second-moment turbulence closure based on weighted spectrum integration. *Theoret. Comput. Fluid Dynamics*, 18:1–26, 2004.

[12] C. Cambon, D. Jeandel, and J. Mathieu. Spectral modelling of homogeneous non-isotropic turbulence. *Journal of Fluid Mechanics*, 104:247–262, 1981.

[13] J. P. Bertoglio and D. Jeandel. A simplified spectral closure for inhomogeneous turbulence: application to the boundary layer. 5^{th} *Symposium on Turbulence Shear Flows, Ed. Springer, Corneil Univ.*, 1986.

[14] M. Lesieur, O. Métais, and P. Comte. *Large-Eddy Simulations of Turbulence.* Cambridge University Press, 2005.

[15] M. Lesieur and O. Metais. New trends in large-eddy simulations of turbulence. *Ann. Rev Journal of Fluid Mechanics*, 28:45–82, 1996.

[16] M. Germano, U. Piomelli, P. Moin, and W. H. Cabot. A dynamic subgrid-scale eddy-viscosity model. *Physics of Fluids*, 3(7):1760–1765, 1992.

[17] B. Chaouat and R. Schiestel. From single-scale turbulence models to multiple-scale and subgrid-scale models by Fourier transform. *To appear in Theoret. Comput. Fluid Dynamics*, 2007.

[18] P. R. Spalart. Strategies for turbulence modelling and simulations. *International Journal of Heat and Fluid Flow*, 21:252–263, 2000.

[19] F. Hamba. A hybrid RANS/LES simulation of turbulent channel flow. *Theoret. Comput. Fluid Dynamics*, 16:387–403, 2003.

[20] L. Temmerman, M. Hadziabdic, M. A. Leschziner, and K. Hanjalic. A hybrid two-layer URANS-LES approach for large eddy simulation at high reynolds numbers. *International Journal of Heat and Fluid Flow*, 26:173–190, 2005.

[21] R. Schiestel and A. Dejoan. Towards a new partially integrated transport model for coarse grid and unsteady turbulent flow simulations. *Theoret. Comput. Fluid Dynamics*, 18:443–468, 2005.

[22] B. Chaouat and R. Schiestel. A new partially integrated transport model for subgrid-scale stresses and dissipation rate for turbulent developing flows. *Physics of Fluids*, 17(6), 2005.

[23] K. Hanjalic, M. Hadziabdic, M. Temmerman, and M. Leschziner. Merging LES and RANS strategies: Zonal or seamless coupling ? In *Direct and Large eddy Simulations 5*, pages 821–831. Ed. by R. Friedrich, B. Geurts and O. Métais, Kluwer Academic, May 2004.

[24] S. Bhushan, Z. U. A. Warsi, and D. K. Walters. Modeling of energy backscatter via an algebraic subgrid-stress model. *AIAA Journal*, 44(4):837–847, 2006.

[25] M. Germano. Turbulence: the filtering approach. *Journal of Fluid Mechanics*, 238:325–336, 1992.

[26] J. O. Hinze. *Turbulence*. Mc. Graw-Hill, 1975.

[27] B. E. Launder and N. Shima. Second moment closure for the near wall sublayer: Development and application. *AIAA Journal*, 27(10):1319–1325, 1989.

[28] M. M. Gibson and B. E. Launder. Ground effects on pressure fluctuations in the atmospheric boundary layer. *Journal of Fluid Mechanics*, 86:491–511, 1978.

[29] I. Befeno and R. Schiestel. Non-equilibrium mixing of turbulence scale using a continuous hybrid RANS/LES approach. *to appear in Flow, Turbulence and Combustion*, 2007.

[30] G. Avalon, G. Casalis, and J. Griffond. Flow instabilities and acoustic resonance of channels with wall injection. AIAA Paper 98–3218, July 1998.

[31] B. Chaouat. Numerical predictions of channel flows with fluid injection using Reynolds stress model. *Journal of Propulsion and Power*, 18(2):295–303, 2002.

[32] B. Chaouat and R. Schiestel. Reynolds stress transport modelling for steady and unsteady channel flows with wall injection. *Journal of Turbulence*, 3:1–15, 2002.

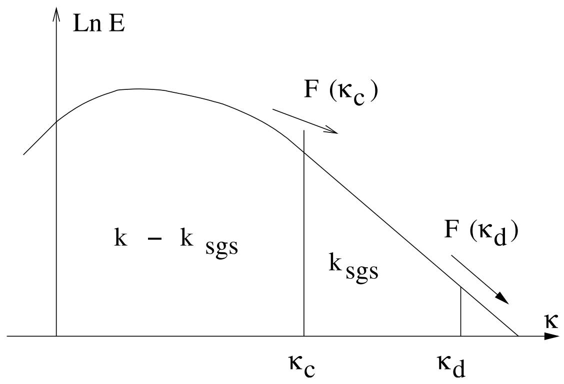

Figure 2: Sketch of spectrum splitting

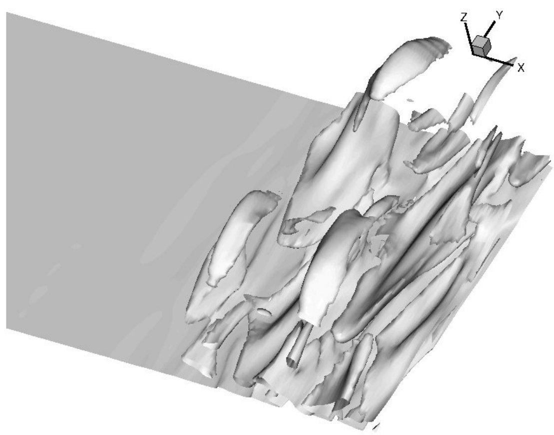

Figure 3: Isosurfaces of instantaneous filtered vorticity vector $\bar{\omega}_i = \epsilon_{ijk}\partial\bar{u}_k/\partial x_j$ in the spanwise direction (i=2) $|\bar{\omega}_2| = 3000$ (1/s). LES simulation [22]. Experimental cold flow setup of Avalon [30].

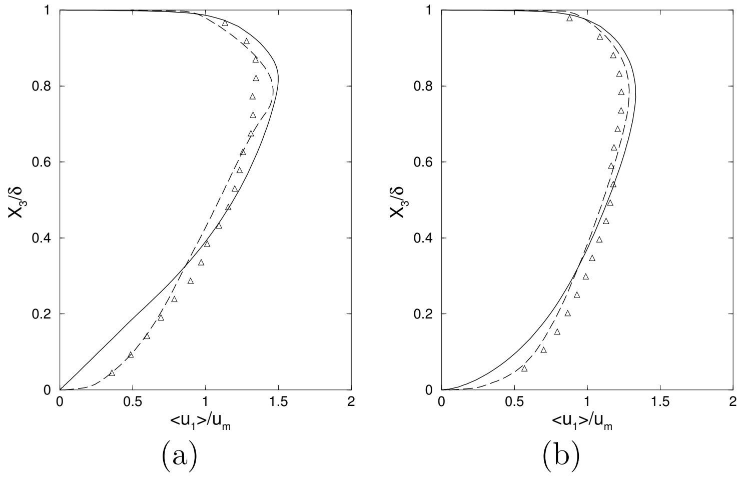

Figure 4: mean velocity profiles normalised by the bulk velocity $\langle u_1 \rangle / u_m$ in different cross sections (a) $x_1 = 40$ cm; (b) 57 cm; —: RSM computation [31]; - - -: LES simulation [22]; Δ: experimental data [30].

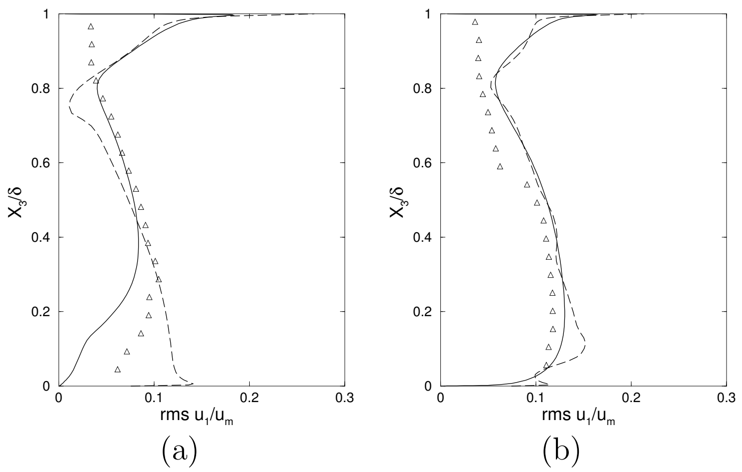

Figure 5: Streamwise turbulent stresses $\langle u_1' u_1' \rangle^{1/2} / u_m$ in different cross sections (a) $x_1 = 40$ cm; (b) 57 cm. —-: RSM computation [31]; - - -: LES simulation [22]; Δ: experimental data [30].